Modelling of surface settlements induced by tunnel excavation using the differential stress release technique

Gioacchino Altamura,* Alberto Burghignoli,** Salvatore Miliziano***

Summary

After a brief hint to recalling the experimental observations of displacements induced by tunnelling in green-field conditions and to the empirical relationships that are usually used to describe such displacements, this paper describes the differential release technique of the forces that originally act on the excavation boundary and the way in which this technique is applied. This technique is used to numerically reproduce the field of displacements induced by the excavation in green field conditions, as a first step to model the interaction between soil and the existing surface structures. This paper includes then the results of the parametric analysis that made it possible to show how the method can be applied to different geometric configurations and geotechnical situations. These results, which are briefly summarised in diagrams and tables, offer guidance on how to use the method. All the tests were carried out in undrained conditions and in terms of effective stresses using a simple perfect elasto-plastic constitutive model with Mohr-Coulomb strength and null dilatancy.

1. Introduction

Excavations in urban environments are becoming more and more widespread and increasingly important in civil engineering. This is because of the need to develop and expand existing infrastructures and fundamental services for the community without disturbing existing surface structures. The excavation of underground tunnels in urban environments is an example of when construction works require studies and careful design not only to ensure stability but also to prevent damages to existing structures. The assessment of potential damages is an important step in design, in particular with buildings of strategical or historical, artistical and monumental importance.

When excavating a tunnel with no existing buildings, i.e. the so-called g*reen-field* condition, a field of displacements is produced on the surface. This field is similar to a trough (settlement trough) that is symmetric to the axial plan of the tunnel and advances with the excavation face [Peck, 1969; New and O'reilly, 1991; Lee *et al.*, 1992]. If structures exist above the future tunnel, the interaction between them and the ground modifies the *green-field* displacements. The damages that may be caused to pre-existing structures is a consequence of the changes in the distribution of the state of stress and strain that occur during excavation and that evolve with it.

These damages generally consist in the production of cracks or in the further widening of existing cracks [Boscardin and Cording, 1989; Burland, 1997; Mair *et al.*, 1996]. Yet, the perturbation of the state of stress and strain in the building-ground system, even in cases in which it does not produce cracks, may give rise to non-visible damages, such as the reduction in the "strength reserves". This can bring about an increase in structural vulnerability in future events like for instance earthquakes [Miliziano and Soccodato, 2003].

The technical literature reports various methods to predict potential damages at different levels of approximation. A simple and widely used method [Burland and Wroth, 1974] evaluates the potential damages by studying the deformation of an extremely simplified model of the structure (an elastic beam) to which the *green-field* displacements are applied in plane strain conditions (i.e. after the passage of the excavation face). The displacements induced in *green-field* conditions may be estimated using empirical relationships that take into account the position and geometry of the tunnel, the nature of the soil and the excavation technique [Peck, 1969; New and O'reilly, 1991; Le, 1992; Lee and Rowe, 1992; Fang *et al.*, 1994]. This method can be used for the initial assessment of the excavation effects, but it does not provide an accurate prediction because it neglects the soil-structure interaction that limits and redistributes the *green-field* displacements more favourably, thus reducing the excavation im-

* PhD, University of Rome "La Sapienza", Department of Structural and Geotechnical Engineering

** Professor, University of Rome "*La Sapienza*", Department of Structural and Geotechnical Engineering

*** Associate Professor, University of Rome "*La Sapienza*", Department of Structural and Geotechnical Engineering

pact on the buildings. Therefore this method gives an overestimated prediction of damages. Nonetheless, this method is widely used in design because it is simple and let identify situations in which appreciable damages are not expected.

In all situations where the level of overestimated damages is high, the soil-structure interaction needs to be thoroughly studied by using models that are closer to reality. To this purpose numerical analysis is a valid tool.

When studying the processes occurring during tunnelling, the most appropriate modelling is the three-dimensional one [BURD *et al.*, 2000; MILIZIANO and SOCCODATO, 2003] because the problem is completely three-dimensional. The displacements field is three-dimensional and evolves as the face advances. The pre-existing buildings, with some exceptions, present also three-dimensional load-bearing structures. The modelling adopted in numerical analysis, however, is often two-dimensional because it is easier to set up and not so heavy in computational terms. In plane strain analysis the three-dimensional nature of the problem is not taken into account, thus overlooking the effects brought about on the structures by the advancing excavation face. The focus is therefore on studying the interaction in a section orthogonal to the tunnel axis when the excavation face is far enough from the section being examined. The 2-D approach requires that the structures of the pre-existing works be parallel and/or orthogonal to the tunnel axis. It also requires the adoption of a plane structure instead of a real 3-D structure with a need to set 2-D/3-D equivalence criteria [MILIZIANO *et al.*, 2002].

Moreover, in choosing to study the interaction by a numerical two-dimensional approach, a problem arises that needs to be solved: how to simulate the excavation process. Literature includes two main sets of techniques, one is based on the application of displacements on the excavation boundary [ROWE and KACK, 1983 a and b; VERRUIJT and BOOKER, 1996; POULOS and LOGANATHAN, 1998; TAMAGNINI *et al.*, 2005] and the other one is based on the reduction of the lithostatic forces that originally act on excavation boundary [STELLEBRASS *et al.*, 1996; NEGRO and DE QUEIROZ, 2000; BURGHIGNOLI *et al.*, 2001]. It is evident that whatever solution chosen to simulate the excavation effects is a numerical "trick" that does not correspond to any physical process taking place during excavation. In addition, the displacements applied at the excavation boundary can cause a simple uniform contraction [VERRUIJT and BOOKER, 1996] or a change in the excavation shape [POULOS and LOGANATHAN, 1998; ROWE and KACK, 1983 a and b]. Instead, in the case of the method of forces reduction, the reduction can occur proportionately to the initial value [NEGRO and DE QUEIROZ, 2000] and can be the same for each point of the tunnel boundary or not. As this is a numerical artifice, the best way of simulating the excavation is the best way of reproducing the surface settlement profile on a plane orthogonal to the tunnel axis far away from the tunnel face. As a matter of fact, before starting the numerical simulation of soil-surface structures interaction, it is necessary to set up a numerical analysis that ensures a good reproduction of the surface settlement in *green-field* condition. It is worth pointing out that the "trick" would be a different one if, for instance, the objective was the evaluation of the final load acting on the lining.

Before to act on the technique adopted to simulate the excavation process, it is interesting to know how the constitutive model can help to improve the reproduction of the surface settlement in *green-field* condition. Some research paper focalize on the effects of advanced constitutive laws implemented in numerical analysis in order to achieve more realistic results on surface settlements profile linked to the construction of shallow tunnels [ADDENBROOKE *et al.*, 1997; BURGHIGNOLI *et al.*, 2001; GUNN, 1992]. All of these works show that the use of advanced constitutive models, associated with the uniform release technique, do not improve significantly the prevision displacement induced on the surface. In other words, the use of advanced constitutive models capable of simulating the strong non-linearity of the mechanical behaviour of the soils could be a complication that is not very useful in achieving the goal that has been set, which is the 2-D analysis reproduction of the correct surface settlements profile experimentally observed in *green-field* condition. The adopted excavation simulation technique must therefore ensure an acceptable reproduction of the displacement induced on the surface in *green-field* conditions. This is a crucial step that deeply impacts on the accuracy of subsequent study of the interaction with the pre-existing structures.

2. Experimental evidence

The experimental data reported in the literature show that the settlement curve in *green-field* conditions in the plane orthogonal to the tunnel axis, at some distance from the face, can be represented by a normal Gaussian probability function [PECK, 1969]. The vertical displacements Sz as a function of the distance y from the axial plane of the tunnel are represented by the following relationship:

$$S_z = S_{z\max} e^{\frac{y^2}{2 \cdot i_y^2}} \qquad (1)$$

This function is characterized by two parameters: the maximum vertical displacement along the tunnel axis, *Szmax*, and the horizontal distance of

the point of inflexion of the curve from the tunnel axis, *iy*. Figure 1 shows a transverse settlement trough normalized with respect to the two parameters that define its shape. Near the tunnel the settlement curve presents an upward concavity (*sagging*), while beyond the point of inflexion the concavity is a downward one (*hogging*).

Many experimental observations have confirmed the validity of the Gaussian relationship irrespective of the nature of the soil, of the excavation technique used and of the drainage conditions [PECK, 1969]. Parameter *iy* depends on the nature of the soil and on the overburden *H/D* [PECK, 1969]. For *H/D*>1 the following correlation can be used [NEW and O'REILLY, 1991]:

$$i_y = k \cdot Z \tag{2}$$

where the dependence on the diameter *D* disappears, the value of *k* varies between 0.2 and 0.3 for sands, between 0.4 and 0.5 for stiff clays and between 0.6 and 0.7 for soft clays. Therefore, once the prevalent nature of the soil has been established, the variation range of *k* and i_y is relatively small.

The maximum settlement *Szmax* depends on geometrical factors, such as diameter and overburden, construction technique and on the mechanical behaviour of the soil, and can be estimated by referencing to literature data in similar conditions or by using correlations that relate it to the volume loss V_L (ratio between the volume of the soil excavated in excess of the nominal volume and the nominal volume of the tunnel), since this can be directly related to the excavation technique. In undrained conditions, the absence of volume changes means that the volume loss V_L is equal to the volume of the surface settlement trough V_S, and the maximum settlement may be calculated through the following relationship:

$$S_{z\max} \cong \frac{V_S}{2.5 \cdot i_y}, \text{ therefore } S_{z\max} \cong \frac{V_L}{2.5 \cdot i_y} \tag{3}$$

As it is very difficult to take measurements, experimental data on the horizontal components of the displacement *Sy* are not so plentiful as the data on vertical displacements. Such components are usually evaluated from the vertical displacement, assuming that the displacement vector is directed towards the centre of the tunnel:

$$S_y = S_z \frac{y}{Z} \tag{4}$$

Figure 2 shows the horizontal displacements on the surface along *y* axis obtained from the previous relationship, normalized with respect to the maximum value, *Symax*.

The horizontal displacement profile produces along *y* axis contraction deformations close to the excavation, and extensile deformations beyond the point of inflexion.

Based on soil characteristics and excavation technique, *green-field* settlement and horizontal displacements at ground level can be estimated on a plane orthogonal to the tunnel axis at sufficient distance from the face (plain strain conditions).

3. Differential stress release technique

Research papers document two main groups of techniques based on plain strain numerical analysis. These techniques can be used to simulate the effects induced on the surface by the excavation of a tunnel. The first group applies the imposition of displacements on the tunnel boundary, while the other reduces the forces acting initially on the tunnel boundary. The differential stress release technique, employed in this paper, belongs to the latter group [BURGHIGNOLI *et al.*, 2001] and consists in the independent release of the vertical (F_{v0}) and horizontal (F_{h0}) components of the force acting initially on the upper (F_{v10}, F_{h10}), and lower (F_{v20}, F_{h20}) parts of the tunnel boundary. This method implies a reduction

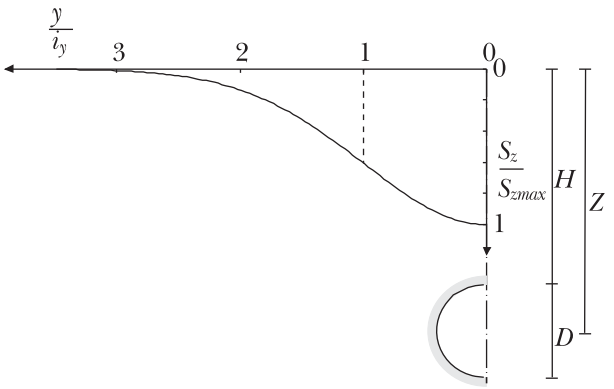

Fig. 1 - Normalized settlements profile.
Fig. 1 - Profilo di subsidenza normalizzato.

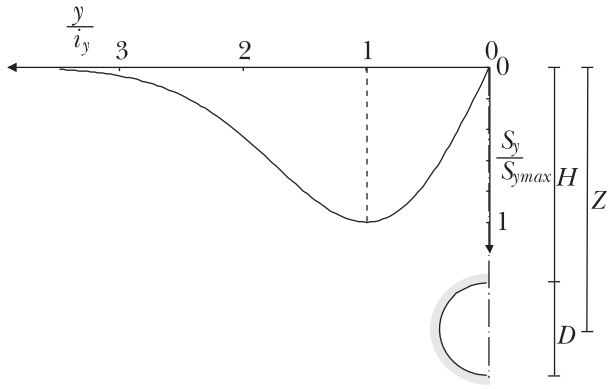

Fig. 2 - Normalized superficial horizontal displacements.
Fig. 2 - Spostamenti orizzontali superficiali normalizzati.

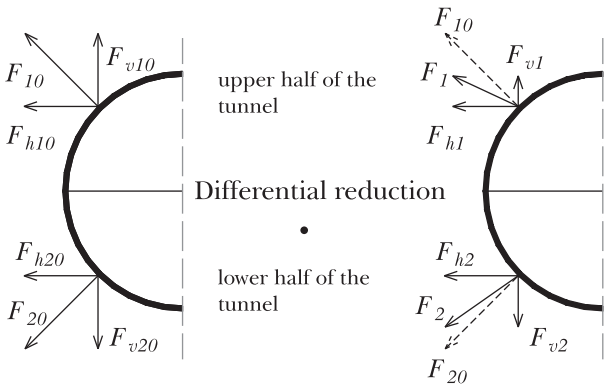

Fig. 3a - Differential reduction of the forces acting on the tunnel boundary.
Fig. 3a - Riduzione differenziale delle forze agenti sul contorno del cavo.

of the magnitude and a rotation of the line of action of the forces that originally act on the tunnel boundary (Fig. 3a). The differential stress release method may be viewed as a generalization of the uniform stress release method, where only the magnitude of all the forces is reduced. In the following, the stress release technique is described in detail.

When using this method, initially are calculated the reactions of the translational restraints applied to the mesh nodes on the tunnel boundary. These restraints are generated when the elements of the mesh located inside the tunnel boundary are removed. Then, the restraints are eliminated while the calculated restraint reactions are applied to the corresponding nodes. (These reactions are the forces corresponding to the initial total state of stress). These first two preliminary steps are characterized by a very light computational workload, since the perturbation applied to the system is very small.

The excavation process (third step) is simulated by progressively reducing these forces. By indicating as P_{sv1} the reduction quota for the vertical components acting initially on the upper boundary of the tunnel F_{v10}, the corresponding values of the forces applied in a generic phase in the analysis are yielded by the following expression:

$$F_{v1}=(1-p_{sv1})\cdot F_{v10} \tag{5}$$

The reduction of the other force components is determined by the following expressions:

$$F_{v1}=(1-p_{sv1}\cdot K_{v2})\cdot F_{v20} \tag{6}$$

$$F_{h1}=(1-p_{sv1}\cdot K_{h1})\cdot F_{h10} \tag{7}$$

$$F_{h2}=(1-p_{sv1}\cdot K_{h2})\cdot F_{h20} \tag{8}$$

where the relative rate at which the forces are reduced is controlled by the numerical values assigned to the three coefficients K_{v2}, K_{h1} and K_{h2}. The product of the generic coefficient K and P_{sv1} is the reduction quota for the generic force component. For instance $P_{sh2}=P_{sv1}\cdot K_{h2}$ is the reduction quota for the horizontal components of the forces initially acting on the lower half of the tunnel. In the analysis results shown in this paper the following condition was systematically set: $K_{h1}=K_{h2}=K_h$; this is the same as reducing in the same way all the horizontal components of the forces. The excavation advancing is simulated by gradually increasing the p_{sv1} value (for instance p_{sv1} = 0.01, 0.02, etc.).

In the fourth step, assuming tentatively values for K_{v2} and K_h, the settlements obtained numerically are compared to the gaussian curve (used as a reference) calculated for the volume of the subsidence curve obtained numerically, in order to select the numerical values for K_{v2} and K_h which provide an acceptable match.

In this paper values of K_{v2} and K_h were accepted when both the following conditions were satisfied:

$$0.9\le \frac{i_{y,num}}{i_{y,gauss}}\le 1.1,$$

$$0.9\le \frac{S_{zmax,num}}{S_{zmax,gauss}}\le 1.1,$$

where the "*num*" refers to the numerical analysis and the "*gauss*" refers to the prediction obtained by the Gaussian curve. No further adjustments were carried out to improve the resulting horizontal displacements. Otherwise, new values of K_{v2} and K_h were selected and the calulation process restart from the third step.

The necessary steps for the application of the differential stress release technique are summarized in the flow chart reported in Figure 3b.

To better select the relative reduction speeds of the individual components of the initial forces, it is useful to know the effect of the reduction of each component on the settlement curve on the surface in terms of vertical and horizontal displacements. To show the effects of the release of the individual components of the initial forces on the numerical results for the surface settlements, an example of specific geometrical and geotechnical conditions[1] is presented in Figure 4. The diagrams in Figures 4a), b), and c) show the settlement curves obtained by unloading just the F_{v1} component, just the F_{v2} component, and finally just the $F_{h1}=F_{h2}=F_h$ component respectively. Each diagram shows, like the results from the numerical analysis, the vertical and horizontal displacements as predicted based on the Gaussian distribution for the same volume loss numerically obtained. The results in the figure refer to the same percentage reduction value for the initial forces. This percentage reduction value and the consequential numerical results are not linked to any physical phenomenon, but are just an example

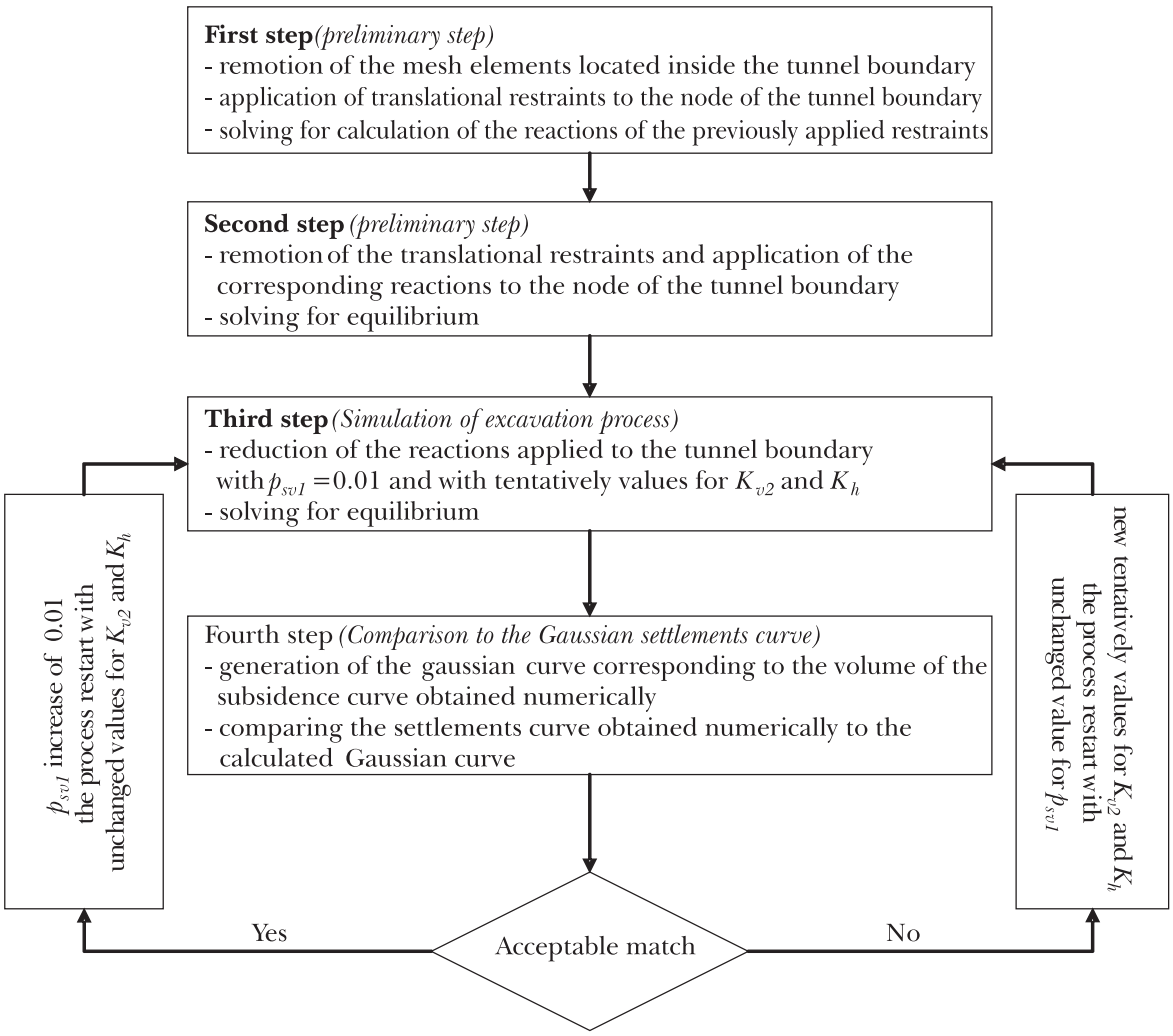

Fig. 3b - Steps for the application of the stress release technique.
Fig. 3b - Passi del processo per l'applicazione del metodo del rilascio differenziale.

showing the effects of the differential release on surface settlements.

It is interesting to note that the unloading of just the F_{v1} component contributes greatly to getting curves that are close to the experimental ones (Fig. 4a). In this case the settlement curve shows the distance from the point of inflexion, which approximately coincides with the one anticipated by the normal distribution function. However the maximum settlement value, S_{zmax}, is larger, and a strong upheaval develops at some distance from the tunnel. The horizontal displacements obtained numerically are appreciably higher than those anticipated by the experimental expressions, even though the overall trend is similar.

The unloading of just the F_{v2} component (Fig.4b) produces curves with trends that are opposite to those already seen for the unloading of just the *Fv1* component. Finally, the settlement curve obtained by unloading only the horizontal components F_h (Fig.4c) is very similar to that obtained for the unloading of F_{v2}. However, it is characterized by small displacements, and the point of the inflexion of the curve is closer to the axial plane of the tunnel. Instead, the horizontal displacement curve presents peaks that do not match those of the Gaussian curve, and a reversal in sign is displayed.

Therefore, in order to get a good representation of the settlement curve and of the horizontal displacement curves, it is necessary to appropriately adjust the amount of simultaneous release for each of the individual forces F_{v1}, F_h, and F_{v2}. Obviously, because of plastic deformation, the effects of each perturbation depend on other individual perturbations. For this reason, the problem needs to be tackled by carrying out numerical analyses where the three components vary at the same time, by adjusting the relative speeds with a trial and error procedure type and by comparing the numerical analysis

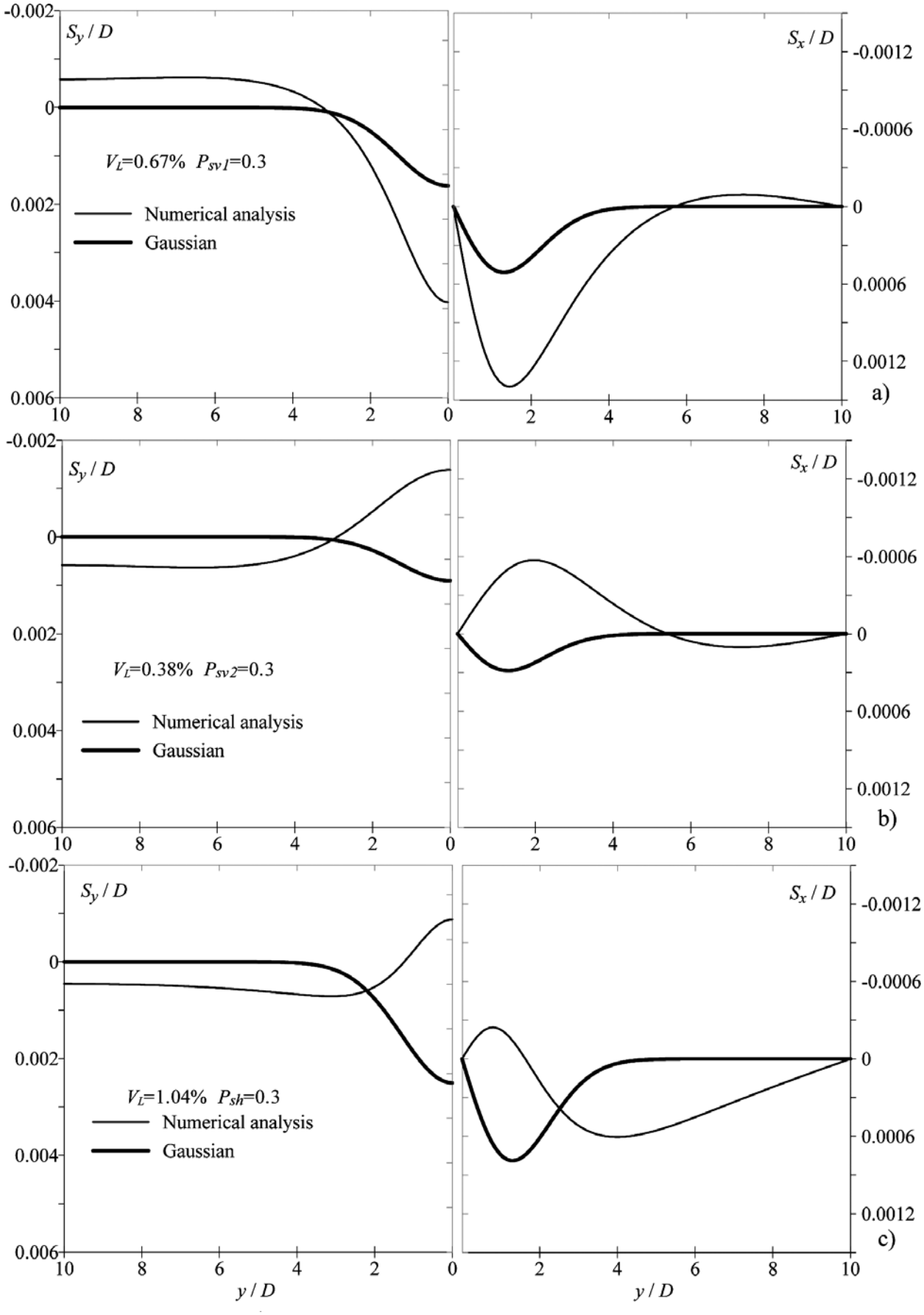

Fig. 4 - Effects of the reduction of the individual components of the force (H=12 m, D=6 m S=42 m and $k0$=0.5).
Fig. 4 - Effetti della riduzione delle singole componenti di forza (H=12 m, D=6 m S=42 m e k0=0.5).

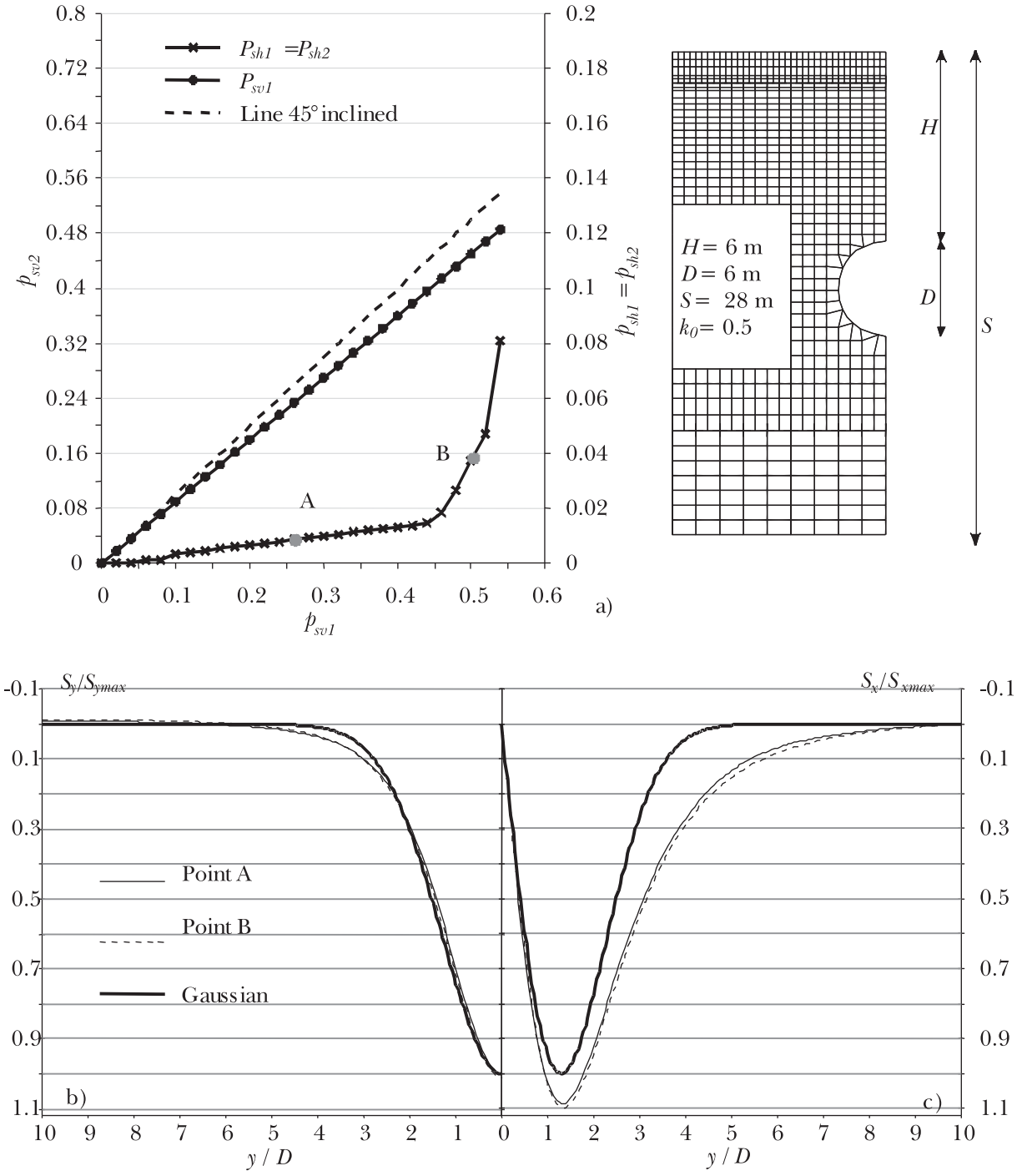

Fig. 5 - Surface displacements obtained using the differential release technique.
Fig. 5 - Andamenti degli spostamenti superficiali ottenuti con la tecnica del rilascio differenziale.

results to the distribution of the reference displacements that are being sought for.

Figure 5 shows the results obtained by applying the differential release technique, where for the sake of simplicity $F_{h1}=F_{h2}=F_h$, again, and the rate of reduction of the vertical components of the forces acting on the lower half of the tunnel (K_{v2} = constant) is unchanged throughout the unloading process. Also in this case the numerical analysis was carried out using a mesh from those used for the parametric analyses (H=6 m, D=6 m, S=28 m and k_0=0.5 k=0.56; the other parameters are reported in the paragraph on numerical analysis). It can be noticed that this technique succeeds in producing, for any value of the unloading amount, *green-field* displacements that are comparable to those derived from the Gaussian distribution.

This substantial coincidence, in the case at hand, comes from the reduction of the vertical forces F_{v2} in a way that is similar to F_{v1} (K_{v2} is a bit

lower than 1). As to the horizontal components, the percentage of reduction is instead rather lower than that of the vertical components. In the earlier unloading stages, when the system is still an elastic field, this reduction is very low, then it increases gradually as the amount of plastic deformations and the extent of the plasticised zones increase. In the final step in the analysis, p_{sv1} equals to 0.54, and p_{sh} equals to 0.08 (the horizontal components of the forces have been reduced by 8% as compared to the 54% reduction for the vertical components of the upper half of the tunnel).

4. Numerical analysis

By using discretization meshes appropriately selected in order to ensure sufficiently accurate solutions and acceptable computational workloads (Fig.6), a parametric study was carried out aimed at verifying the applicability of the differential release technique in different geometric and geotechnical conditions. The results are summarised in tables and diagrams, which may be a useful guide for implementing this technique.

The dimensions of the meshes vary according to the multiplication factors of the tunnel diameter. These factors are chosen appropriately. The transverse dimension of the grid is kept constantly equal to ten diameters (as suggested in literature to minimize the effects of the restraints imposed on the mesh side boundaries). The horizontal kinematic restraints are applied at the mesh vertical boundaries, while vertical and horizontal restraints are applied at the grid base. The number of elements used in the analysis depends on the specific geometric configuration being analysed. A typical discretization density is shown in Figure 6. For further details refer to ALTAMURA [2001].

The numerical analysis was carried out using FLAC, a commercial finite difference calculation code [ITASCA, 2002]. Nine geometric configurations different in terms of overburden, H, and thickness of deformable soil, S, were taken into account. Each of them was studied three times for the three values for the coefficient at rest of earth pressure, k_o.

Therefore a total of 27 analyses were carried out. The geometry of the problem was defined by introducing two non-dimensional parameters:

$$r_1=\frac{H}{D} \text{ and } r_2=\left[\frac{S}{H+\frac{D}{2}}\right] \tag{9}$$

They respectively represent the overburden normalised against the tunnel diameter and the thickness of the deformable soil normalised against the tunnel axis depth.

Values of 1, 2, and 3 were adopted for r_1 considering that the tunnels examined in this study are shallow tunnels for which r_1 values are small. Because the tunnel diameter was set to 6 m, the corresponding values used for H were 6, 12, and 18 m.

As far as the deformable soil thickness is concerned, five different values were adopted (18, 28, 42, 70, and 105 m). They match the values for r_2 shown in Table I.

This choice has made it possible to reduce the number of meshes to be analysed and obtain three

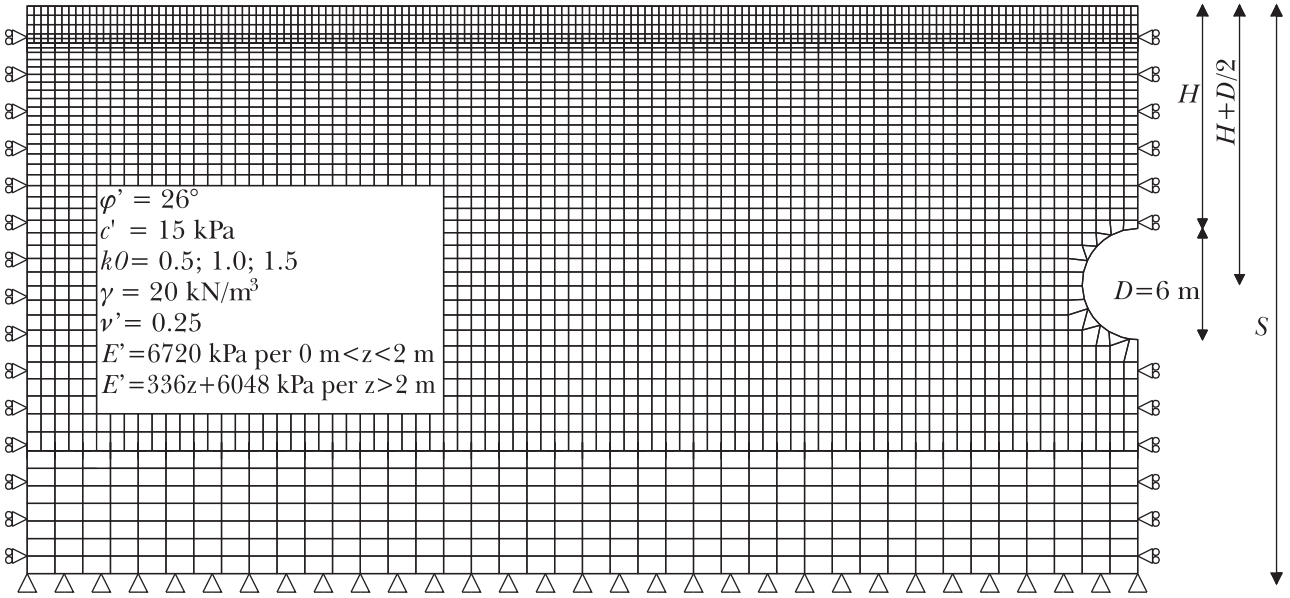

Fig. 6 - Typical density of the meshes used and numerical values for the physical and mechanical parameters of the soil.
Fig. 6 - Tipica densità dei reticoli impiegati e valori numerici dei parametri fisici e meccanici del terreno.

Tab. I – Values for the r_2.parameter associated to the geometric configuration.
Tab. I – Valori del parametro r_2 corrispondenti alle configurazioni geometriche studiate.

		H+D/2		
		9m	*15m*	*21m*
S	18*m*	2,0	–	–
	28*m*	3,1	1,87	–
	42*m*	4,7	2,8	2,0
	70*m*	–	4,7	3,3
	105*m*	–	–	5,0

sets of three values for the r_2 ratio of values close to 2, 3, and 5.

As explained in the introduction, the choice for a simple perfect elasto-plastic constitutive model with a Mohr-Coulomb failure criterion was made for the soil for the sake of simplicity and considering the objectives being pursued, that is the best reproduction of the surface settlement profile on a plane orthogonal to the tunnel axis at a certain distance from the tunnel face, in *green-field* condition, using bi-dimensional numerical analyses. Dilatancy was zero and Young's modulus increased linearly with depth. The initial distribution of the pore pressures is hydrostatic, with a free surface coinciding with the upper boundary of the mesh. All of the analyses were carried out in undrained conditions and in terms of effective stresses. The numerical values for the geotechnical parameters, which are typical of a slightly overconsolidated clay, are shown in Figure 6, and the k value used to evaluate the horizontal position of the point of inflection for the Gaussian curve, i_y, is assumed to be 0.56.

The only geotechnical parameter that has been varied for different analyses is the coefficient at rest of earth pressure k_0, to which the values of 0.5, 1.0, and 1.5 are alternately attributed. As a matter of fact, previous numerical studies have demonstrated that strength parameters, like the deformability parameters, have no significant influence on the shape of the settlement trough, at least in the early unloading stages and until the plastic deformation becomes significant [ALTAMURA, 2001].

5. Results description and comments

The results obtained are summarized in Figure 7, where p_{sv2} and *psh* are shown as a function of p_{sv1}. This enabled us to obtain displacements on the surface that were in agreement with the Gaussian curve used as a reference for variations in the geometry of the problem (r_1 e r_2) and of *ko*. In particular, each column is characterized by a fixed value for the ratio r_1 and each row by a constant value for the ratio r_2. Each diagram presents three curves related to the unloading percentage of the horizontal components, corresponding to the three different values assumed for k_o.

As pointed out earlier in the comments on Figure 5, during the unloading process the reduction in the vertical components at the lower half of the tunnel may occur at constant speed and is only slightly different from that in the components acting on the upper half. As far as the horizontal components are concerned, the beginning of the unloading process is characterized by relatively modest reductions. Then, after a marked bend, the reduction speed of these components varies abruptly. In analysing the development of the strain and stress state, the strong non-linearity of the trends of *psh*, has been matched to the shift from mainly elastic global behaviours to the marked development of plastic deformations.

Please note that, in some cases, after an initial reduction, it is necessary to increase again the horizontal components of the forces. This circumstance, which does not carry any physical meaning, emphasizes what was previously said about the empirical nature of the method. In all the cases, however, the increase in the horizontal components, when added vectorially to the reductions of the other components, continue to produce reductions in the module of the resulting force applied to the tunnel boundary.

By making the trends of p_{sh} linear (Fig.7), the results obtained can be summarized by the values of K_h before and after the *sharp bend* (K_h and K_h', respectively), by the value of *psv1* where the *sharp bend* (p_{sv1}*) is positioned, and by the coefficient K_{v2}. The results are summarized in Table II and in Figure 8.

Having set the geometry of the problem, which is synthetically expressed by the numerical values for the parameters r_1 and r_2, and knowing the value of k_0, the results reported in Figure 8 allow us to estimate the curves that interpolate the values for the 4 parameters (K_{v2}, K_h, K_h' e p_{sv1}*) defining the specific modality of reduction for the forces necessary to obtain numerical *green-field* results that are close to a Gaussian distribution. Alternatively, the results in numerical form (Tab. II) can be used resorting to interpolation for the situations that are not directly investigated.

The parameter K_{v2} does not vary greatly. It takes on values between 0.8 and 1.05. Once the geo-metry is set, this parameter is independent from the value of k_0. Moreover, the dependence of K_{v2} on r_2 decreases as r_1 increases. Viceversa, as r_2 increases, its dependence on r_1 tends to disappear

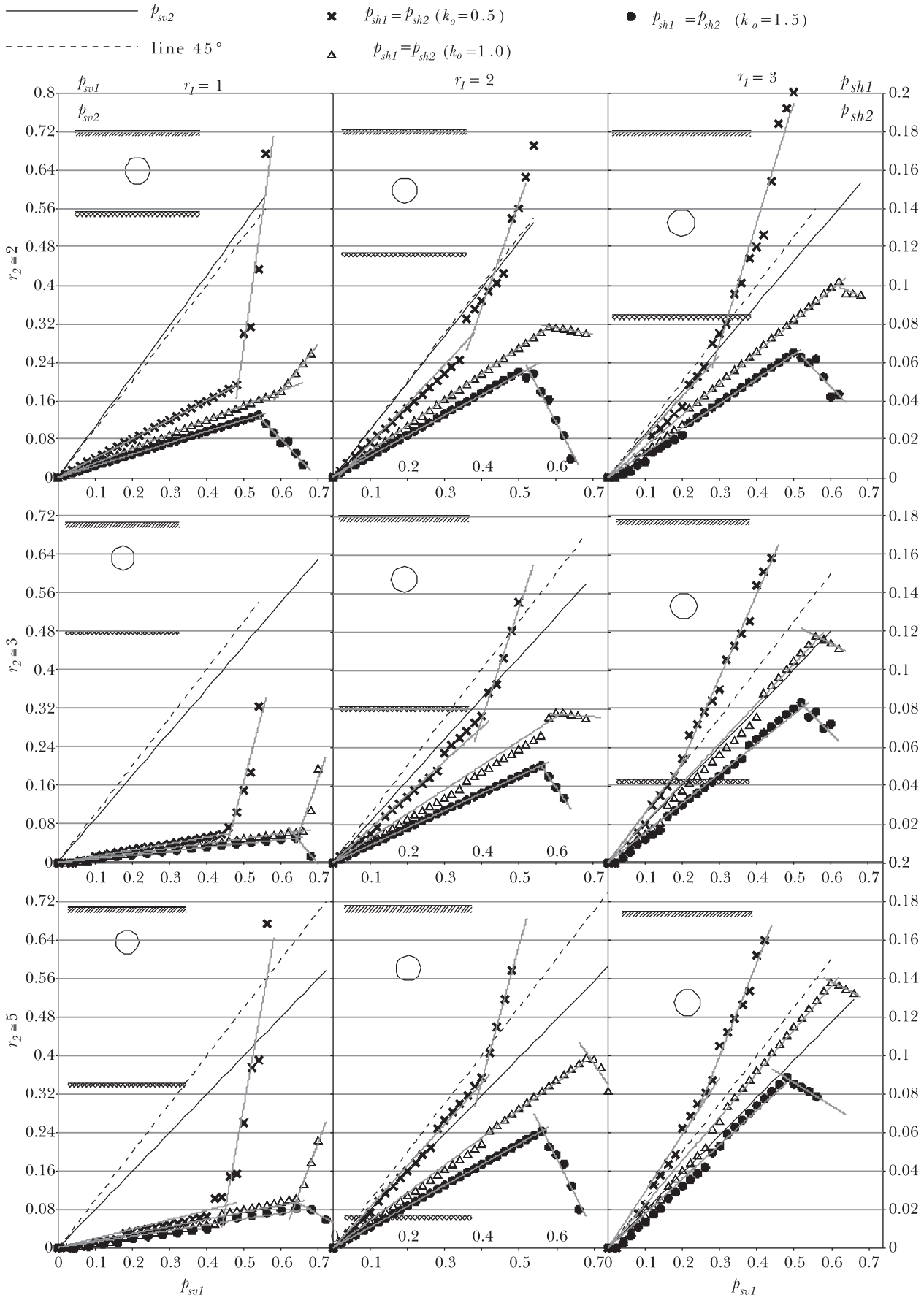

Fig. 7 – Results of the analyses.
Fig.7 - Risultati delle analisi.

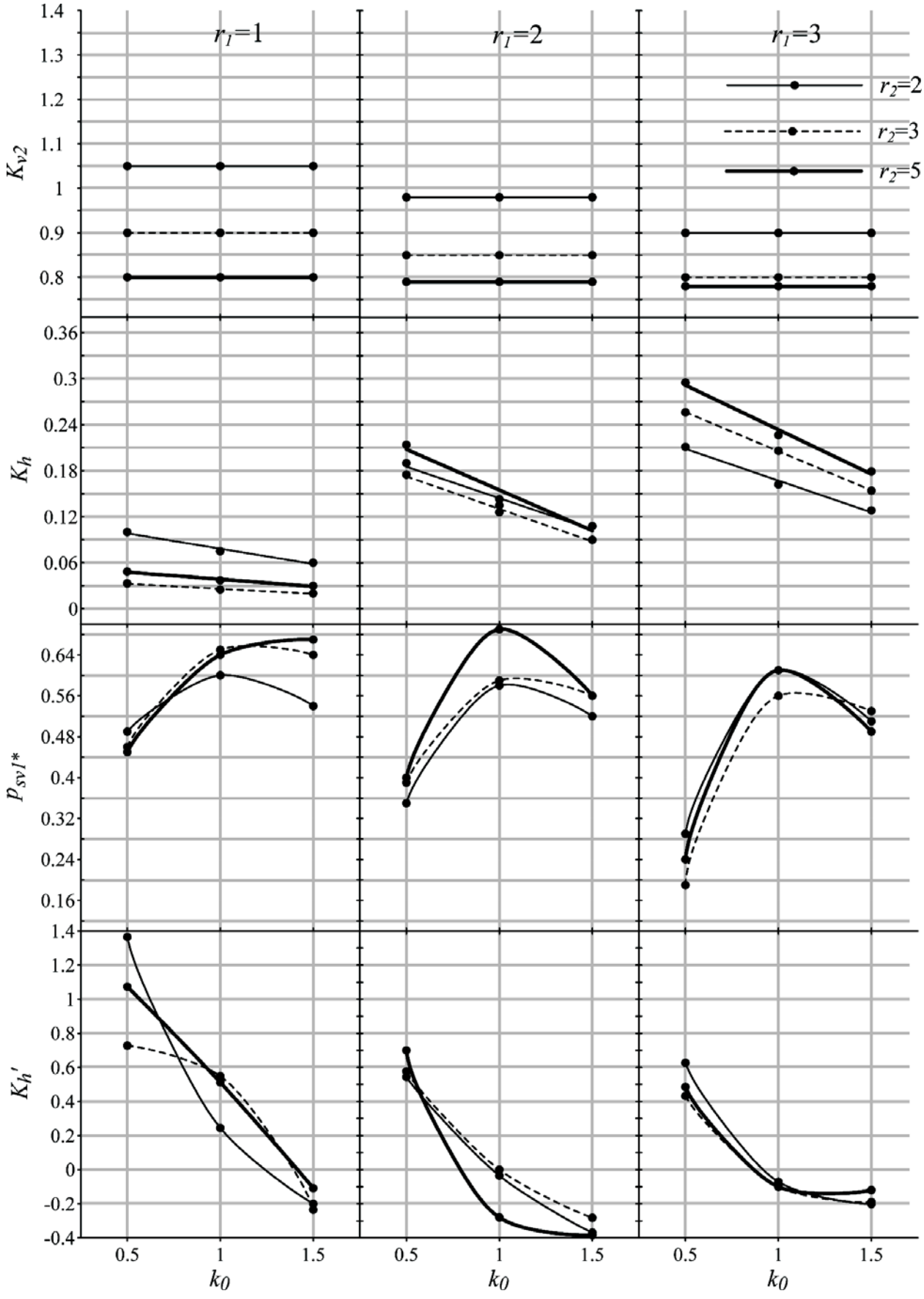

Fig.8 - Summary representation of results.
Fig.8 - Rappresentazione di sintesi dei risultati ottenuti.

Tab. II - Summary of results.
Tab. II - Quadro riassuntivo dei risultati ottenuti.

	$r_2\rightarrow$	≅2				≅3				≅5			
$r_1\downarrow$	k_0	K_{v2}	K_h	p_{sv1}*	K'_h	K_{v2}	K_h	p_{sv1}*	K'_h	K_{v2}	K_h	p_{sv1}*	K'_h
1	**0.5**	1.05	0.1	0.49	1.365	0.9	0.033	0.46	0.728	0.8	0.048	0.45	1.073
	1	1.05	0.075	0.6	0.245	0.9	0.025	0.65	0.549	0.8	0.037	0.64	0.512
	1.5	1.05	0.06	0.54	-0.2	0.9	0.02	0.64	-0.235	0.8	0.03	0.67	-0.108
2	**0.5**	0.98	0.19	0.35	0.544	0.85	0.175	0.39	0.577	0.79	0.214	0.4	0.7
	1	0.98	0.135	0.58	-0.035	0.85	0.126	0.59	0	0.79	0.143	0.69	-0.28
	1.5	0.98	0.108	0.52	-0.369	0.85	0.09	0.56	-0.282	0.79	0.108	0.56	-0.384
3	**0.5**	0.9	0.211	0.29	0.627	0.8	0.256	0.19	0.433	0.78	0.295	0.24	0.485
	1	0.9	0.162	0.61	-0.071	0.8	0.206	0.56	-0.1	0.78	0.226	0.61	-0.1
	1.5	0.9	0.28	0.51	-0.201	0.8	0.154	0.53	-0.19	0.78	0.179	0.49	-0.119

(Fig. 9). In other terms, as the tunnel depth increases, the influence of the deformable soil thickness tends to decrease. Moreover, if the latter assumes high values, the parameter K_{v2} tends to assume a constant value of about 0.8. The values of K_{v2} greater than one that are obtained for shallow tunnels and for small deformable soil thickness are necessary to offset the marked settlement along the axis and the upheaval at a distance from the axis of simmetry that result from the unloading of the vertical components of just the upper half of the tunnel (Fig. 4).

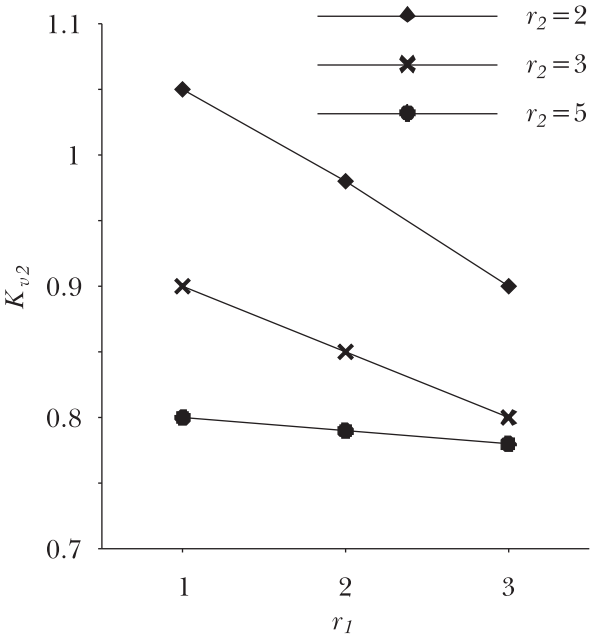

Fig. 9 - Parameter K_{v2} as a function of r_1 e r_2.
Fig. 9 - Andamento del parametro K_{v2} in funzione di r_1 e r_2.

Parameter K_h assumes values between 0.05 and 0.30, and it is always appreciably less than one. K_h takes on higher values as the tunnel depth increases.

The transition from mainly elastic conditions to conditions characterized by a major development of plastic deformations, as mentioned above, is identified by parameter p_{sv1}*. It can be noticed that the amount of the unloading that supports the system in plastic conditions is higher for the initial isotropic states of stress (k_o=1), as a consequence of the initially large distance between the initial state of stress and the strength criterion.

The parameter K_h' decreases rapidly as k_0 increases, and it takes on very high values similar to those of K_{v2} when the coefficient at rest of earth pressure is 0.5. For values of k_0 greater than or equal to 1, K_h' may take on negative values.

6. Conclusions

When assessing the damages caused by the excavation of shallow tunnels on pre-existing buildings, it is often necessary to thoroughly study the soil-structure interaction. For this purpose we need numerical models capable of reproducing the field of surface displacements induced in *green-field* condition. Three-dimensional models are the best when it comes to studying the processes that occur during tunnel excavation because the field of dis-

placements, which evolves as the face advances, has markedly 3-D characteristics, just like the bearing structures of the pre-existing buildings. Yet, the models used in designing are often two-dimensional because they are simpler to set up and less burdensome in computational terms. In plane strain analysis, the three-dimensional nature of the problem is of course ignored, so the effects of the advancing excavation face on buildings are overlooked. The focus is on studying the interaction in a section orthogonal to the tunnel axis when the excavation face has moved far ahead. Moreover, it is necessary to identify excavation simulation methods that will reproduce the *green-field* displacements in accordance with experimental evidence.

This paper has provided a detailed description of the differential stress release technique, which is able to easily simulate the field of displacements induced at ground level by the construction of a tunnel. This is made possible thanks to the indipendent reduction of the vertical and horizontal components of the forces acting at the tunnel boundary before the excavation takes place. This paper has also presented the results of the parametric numerical analyses which were used to demonstrate the applicability of the method to various geometric configurations and different value of coefficient at rest of earth pressure k_0.

The results obtained, which are summarized concisely in diagrams and tables, provide guidance to the use of the method in bedding and mechanical conditions that are different from those considered in the parametric study that was carried out.

The technique of excavation simulation hereby presented ensures the reproduction of surface displacements in accordance with the experimental data in *green-field* conditions in 2-D numerical analyses in a better way than other methods, such as the uniform release technique. This is a very important and preliminary step to improve the accuracy of the numerical study of soil and pre-existing structures interaction due to tunnelling.

Notes

[1] The analysis was carried out by modelling the soil as an elasto-plastic continuum and by using one of the discretization meshes taken into account in the parametric analysis (Cfr. §. Numerical Analyses), which is characterized by H=12 m; D=6 m and by the thickness of the mesh, S, of 42 m (where S is the thickness of deformable soil). The value for k_0 is assumed to be 0.5; the value 0.56 is adopted for the parameter k, which is typical of a slightly overconsolidated clay. The numerical values of the other physical and mechanical parameters used are reported in the paragraph on numerical analyses.

References

ADDENBROOKE T.I., POTTS D.M., PUZRIN A.M. (1997) - *The influence of pre-failure soil stiffness on the numerical analysis of tunnel construction.* Géotechnique, 47, n. 2, pp. 693-712.

ALTAMURA G. (2001) - *Modellazione del campo di spostamenti prodotto dallo scavo di gallerie finalizzata alla valutazione del danno indotto sugli edifici preesistenti.* Tesi di laurea in meccanica delle terre, Università di Roma "La Sapienza", Facoltà di Ingegneria.

BOSCARDIN D.M., CORDING E.J. (1989) - *Building response to excavation induced settlement*. ASCE Journal of Geotechnical Engineering, 115, pp. 1-21.

BURD H.J., HOULSBY G.T., AUGARDE C.E., LIU G. (2000) - *Modelling the effects on masonry buildings of tunnelling-induced settlement*. ICE Proceedings Geotechnical Engineering, 143, n. 1, pp. 17-29.

BURGHIGNOLI A., MILIZIANO S., SOCCODATO F.M. (2001) - *Prediction of ground settlements due to tunnelling in clayey soils using advanced constitutive soil model: a numerical study*. Int Symp. on Modern Tunneling Science and Technology, Kyoto, vol. I, pp. 115-120.

BURGHIGNOLI A., MAGLIOCCHETTI A., MILIZIANO S., SOCCODATO F.M. (2001) - *A simple technique to improve the prediction of surface displacement profiles due to shallow tunnel construction*. Int Symp. on Modern Tunneling Science and Technology, Kyoto, vol. I, pp. 105-110.

BURLAND J.B. (1997) - *Assesment of risk of damage to buildings due to tunnelling and excavations.* Proc. 1st Int. Conf. On Earthquake Geothecnical Engineering, Tokyo, Balkema, 3, pp. 1189-1201.

BURLAND J.B., Wroth C.P. (1974) - *Settlement of buildings and associated damage.* Conference on Settlement of Structures, Cambridge, Pentech Press, pp. 611-654.

FANG Y.S., LIN J.S., SU C.S. (1994) - *An estimation of ground settlement due to shield tunnelling by the Peck-Fujita method* - Canadian Geotechnical Journal, n. 31, 1994, pp.431-441.

GUNN M.J. (1992) - *The prediction of surface settlement profiles due to tunnelling.* Predictive Soil Mechanics, Oxford, pp. 304-313.

ITASCA (2002) – *FLAC 4.0 User's Manual.* Itasca Counsulting Group, Inc. Minneapolis, Minnesota, USA.

LEE K.M., ROWE R.K., LO K.Y. (1992) - *Settlement owing to tunnelling. I. Estimating the gap parameter*. Canadian Geotechnical Journal, 22, pp. 929-940.

LEE K.M., ROWE R.K. (1992) - *Settlement owing to tunnelling. II. Estimating the gap parameter*. Canadian Geotechnical Journal, 22, pp. 940-953.

MAIR R.J., TAYLOR R.N., BURLAND J.B. (1996) - *Prediction of ground movements and assessment of risk of building damage due to bored tunnel.* Geotechnical

Aspects of Underground in Soft Ground, London, Balkema, pp. 713-718.

MILIZIANO S., SOCCODATO F.M., BURGHIGNOLI A. (2002) - *Evaluation of damage in masonry buildings due to tunnelling in cleyey soils*. Int. Symp, Geotechnical Aspect of Underground in Soft Ground, Toulouse, pp. 335-340.

MILIZIANO S., SOCCODATO F.M. (2003) - *Modellazione 2D e 3D di gallerie in ambiente urbano: valutazione del danno indotto sugli edifici in muratura*. XXI Convegno Nazionale di Geotecnica, Opere geotecniche in ambiente urbano, L'Aquila, Settembre 2003.

NEGRO A., DE QUEIROZ P.I.B. (2000) - *Prediction and performance: a review of a numerical analyses for tunnels*. Geotechnical Aspects of Underground in Soft Ground, Tokyo.

NEW B.M., O'REILLY M.P. (1991) - *Tunnelling induced ground movements: predicting their magnitude and effects*. Ground Movements and Structures, Cardiff, J.D.Jeddes, 4, pp. 671-691.

PECK R.B. (1969) - *Deep excavations and tunnelling in soft ground*. Proc. of 7th Int. Conf. Soil Mech., Mexico, State of the Art 3, pp. 225-290.

POULOS H.G., LOGANATHAN N. (1998) - *Analytical prediction for tunnelling induced ground movements in clays*. Journal of Geotechnical and Geonvironmental Engineering, 124, 9, pp. 846-856.

ROWE R.K., KACK G.J. (1983 a) - *A method of estimating surface settlement above tunnels constructed in soft ground*. Canadian Geotechnical Journal, 20, 1, pp. 11-22.

ROWE R.K., KACK G.J. (1983 b) - *A theoretical examination of the settlements induced by tunnelling: four case histories*. Canadian Geotechnical Journal, 20, 1, pp. 299-314.

STALLEBRASS S.E., GRANT R.J., TAYLOR R.N. (1996) - *A finite element study of ground movements measured in centrifuge model tests of tunnels*. Geotechnical Aspects of Underground in Soft Ground, London, Balkema, pp. 595-600.

TAMAGNINI C., MIRIANO C., SELLARI E., CIPOLLONE N. (2005) - *Two-dimensional FE analysis of ground movements induced by shield tunnelling: the role of tunnel ovalization*. Rivista Italiana di Geotecnica RIG, n. 1/05, pp. 11-33.

VERRUIJT A., BOOKER J.R. (1996) - *Surface settlements due to deformation of a tunnel in an elastic half plane*. Géotechnique, 46, n. 4, pp. 753-756.

Notations

φ'	friction angle
c'	effective cohesion
D	diameter of the tunnel
F_{h0}	initial horizontal constraint reaction
F_{h10}	initial horizontal constraint reaction of the upper half of the tunnel
F_{h20}	initial horizontal constraint reaction of the lower half of the tunnel
F_{v0}	initial vertical constraint reaction
F_{v10}	initial vertical constraint reaction of the upper half of the tunnel
F_{v20}	initial vertical constraint reaction of the lower half of the tunnel
H	thickness of the overburden
i_y	horizontal distance from the tunnel axis of the point of inflexion of the settlement trough
k	parameter for the trough breadth
k_0	coefficient of earth pressure at rest
K_h	reduction speed in the horizontal component of the forces applied to the boundary of the excavation, for values lower than psv1*
K_h'	reduction speed in the horizontal component of the forces applied to the boundary of the excavation, once the value of p_{sv1}* is exceeded
K_{h1}	reduction speed in the horizontal component of the forces applied to the upper boundary of the excavation
K_{h2}	reduction speed in the horizontal component of the forces applied to the boundary of the lower half of the tunnel
K_{v1}	reduction speed of the vertical components of the forces applied to the boundary of the lower half of the tunnel
p_{sh}	the quota of reduction for the horizontal components of the forces acting initially on the boundary of tunnel
p_{sv1}	the quota of reduction for the vertical components of the forces acting initially on the upper boundary of tunnel
p_{sv1*}	the critical quota of reduction for the vertical components of the forces acting initially on the upper boundary of the tunnel
r_1	overburden normalized against the tunnel diameter
r_2	thickness of the deformable soil normalised against the depth of the tunnel axis
S	thickness of the deformable soil where the tunnel is excavated
S_y	horizontal displacement
S_z	vertical displacement (settlement)
S_{zmax}	maximum vertical displacement
S_{ymax}	maximum horizontal displacement
V_L	volume lost
V_S	volume of the settlement trough
y	transverse direction to the tunnel axis
Z	depth of the tunnel axis

Modellazione della subsidenza indotta dallo scavo di gallerie mediante la tecnica del rilascio differenziale

Sommario

Nel corpo dell'articolo, dopo un breve richiamo a quanto osservato sperimentalmente in termini di spostamenti indotti dallo scavo di gallerie in condizioni di green-field e alle relazioni empiriche usualmente adottate nel descrivere tali spostamenti, si illustra la tecnica del rilascio differenziale delle forze agenti originariamente al contorno del cavo. Questa tecnica è adottata per riprodurre numericamente il campo di spostamenti indotto dallo scavo in superficie al fine di modellare l'interazione terreno-stutture preesistenti in superficie. A seguire, si riportano i risultati delle analisi parametriche sviluppate che hanno permesso di evidenziare l'applicabilità del metodo a diverse configurazioni geometriche e situazioni geotecniche. I risultati ottenuti, riassunti sinteticamente sotto forma grafica e tabellare, forniscono una guida all'uso del metodo. Tutte le analisi sono state eseguite in condizioni non drenate e in termini di tensioni efficaci, impiegando un semplice legame costitutivo elasto-plastico perfetto con criterio di resistenza di Mohr-Coulomb e dilatanza nulla.